IONOSONDE NETWORK ADVISORY GROUP (INAG)*

IONOSPHERIC STATION INFORMATION BULLETIN NO. 52**

From the Chairman

Comment from the New Chairman, P J Wilkinson

Professor Gledhill's unexpected death left the chair of INAG vacant. Dr Rishbeth, the Chairman for URSI Commission G, asked me if I would take up this position until the next URSI General Assembly and I agreed. This change in the chair does not affect any of the other offices associated with INAG or its operation.

In the rest of this note I will outline some areas I believe INAG should consider. The world ionosonde network will change a great deal over the next decade and INAG will need to respond rapidly to these changes if it is to continue to offer useful advice.

New types of ionosondes will operate in the worldwide network. THE IPS-42 was the first of the modem ionosondes to gain international acceptance. Now computer based ionosondes are becoming more prevalant. The Lowell digisonde will soon be used widely in the northern hemisphere and in Australia a new computer based ionosonde is also being developed. Neither of these systems record ionograms on film, making archiving and exchanging ionograms between scientists different and possibly more difficult. Workable guidelines for data exchange are needed.

Computer scaling of ionograms will become commonplace. Many will be unhappy with this development; however, it is a reality because it is economically desirable and because it guarantees rapid access to the data. INAG will have to offer practical guidelines on what to expect from computer scaled data because impractical standards will ensure fragmentation of the network. It is still essential that data from all ionosondes within the worldwide ionosonde network are readily available for scientific study and that researchers do not have to know where the data come from before they can use them with confidence. This will raise important issues, such as; are scaling letters useful? How useful are scaled parameters when real height electron density distribution estimates are available?

However, these are minor issues compared with the shift in reasons for operating ionosondes. At the time of INAG's inception most ionosondes were operated solely to collect data. Often data usage was independent of collection so INAG was the only tangible guidance available for ionosonde operation and ionogram scaling. This emphasis has changed. Economic realities mean ionosonde networks are operated for dedicated purposes; for instance, to collect ionospheric information to support an HF application. Data from such networks will reflect the primary objective and may never be archived. INAG needs to offer an open forum for discussing archival requirements in data. Ionospheric scientists will need to show how application oriented data can be made more reliable and worth archiving for future study. In essence, INAG must discuss what extra care Is required to make the data valuable as well as show the data collector this cost is reasonable.

A second issue arising here is the disappearance of ionosonde stations that cannot show some immediate economic return. INAG must have sensible advice to office here. To this end, the INAG address list could well be a useful resource for identifying groups who are interested in using ionospheric data. Over the next year the INAG mailing list will be upgraded to ensure that the bulletin is reaching the correct people.

Over the next decade several major international programmes will profit from good ionospheric data inputs. Data from ionosondes are now seen as a useful resource by modellers because of the global coverage. This interest will soon dwindle if the data prove too hard to obtain in a timely fashion. Currently the most important of these programmes is the World Ionosphere Thermosphere Study, WITS.

INAG must adopt a strong role supporting international programmes. Using the bulletin these programmes will be advertised and campaigns will be highlighted. Campaigns are occasions when ionospheric data can have an immediate scientific impact provided the data are collected into global data sets rapidly. Another concern will be to upgrade the current list of all ionosonde sites - both open sites and closed sites. in later bulletins readers will be asked to assist in establishing where stations are and what their current status is.

Another important task for INAG will be to establish strong ties with two other URSI Working Groups; Ionospheric Informatics and Ionospheric Modelling. Both groups have objectives that are important for INAG.

Finally, INAG is always interested in obtaining submissions for the bulletin. If you have submissions or wish to express an interest in INAG please contact the Chairman at the address below. Note, this is a new address.

Dr Phil Wilkinson, INAG CHAIRMAN
IPS Radio and Space Services,
P 0 Box 702
Darlinghurst, NSW 2010
AUSTRALIA.

1. Obituary - J A Gledhill

John Alan Gledhill was born at Littleborough, Lancashire, England on 1 January 1920 and died on 19 June 1988, at the age of 68. At the age of fourteen he emigrated with his parents to South Africa, and after matriculating, began his long association with the then Rhodes University College. Whilst lecturing at Rhodes, he obtained an MSc degree in Chemistry and a PhD degree in Physics from the University of South Africa. He then completed a PhD degree in Chemistry at Yale University, before returning to the Chemistry Department at Rhodes.

In 1954 he reverted to Physics when he was appointed Professor and Head of the Department of Physics at Rhodes University, a post he held for 30 years. In 1984 he was appointed Director of the Hermann Ohlthaver Institute for Aeronomy at Rhodes University.

He has earned worldwide recognition as a research scientist through his prodigious publications in international journals and papers delivered at international conferences. His interests were extremely broad and he and a co-worker were among the first to suggest and confirm the presence of a 2000 K layer 200 to 300 kilometres above the surface of the earth. In 1967 he predicted that the magnetosphere of the planet Jupiter is spun out into the shape of a disc by the planet's rapid rotation. This fact was subsequently confirmed by the US Spacecraft Pioneer 10, in 1974 and is now referred to as the Gledhill disc. His name will always remain synonymous with the effects of particle precipitation upon the ionosphere in the South Atlantic Anomaly Region.

It was typical of Jack Gledhill that he was not content merely with research. He also involved himself in the administration of global research projects, not only as a valued member of many commissions, but also in working groups. He was Chairman of the International Working Group of the 1976 Antarctic and Southern Hemisphere Aeronomy Year, and was Chairman of the Interdivisional Commission of Antarctic Research. In 1984 he succeeded Roy Piggott as Chairman of INAG.

Although very active at the international level he did not neglect to channel some of his boundless energy into areas where it was needed in South Africa. Prof Gledhill served for 20 years on the Joint Matriculation Board and has been active on many of its committees, serving a distinguished two year term as Chairman. He was in his 27th year as Director of the Ionospheric Research Programme of the South African National Antarctic Expeditions and was a member of the Prime Minister's Scientific Advisory Council for 7 years.

His interests as a scholar extended far beyond the boundaries of science. He served on the Board of Historic Grahamstown for 12 years of which he was Vice-Chairman for 8 years. He was also the editor of the Annals of the Grahamstown Historical Society. He and his wife, Or E A Gledhill, have written a book, "In the Steps of Piet Retief", published in 1980.

He was the Treasurer of Abalizi (the Xhosa translation means - The people who help), an organisation which raised funds and built low cost housing for the under-privileged peoples of the Grahamstown area - in all 400 houses were built. This scheme has now spread throughout the Eastern Cape.

However, while many may stand in awe of his stature in the Scientific Community, it is the personality of Jack Gledhill that will remain most vivid in the hearts and minds of those that knew him. He had an outstanding ability to make friends which acknowledged no barriers of language, race or social standing. His wit was well known and there was seemingly no situation that could not evoke from him an interesting and amusing story garnered from his exceptional memory and wealth of experience. He was a man of immense energy who was ever busy, but always had the time to chat with the humblest of his students or employees.

Those of us who knew and worked with "Prof" record his passing with sorrow, but with great affection for he enriched our lives with his exceptional personality, his rare gift of communication at all levels and above all the ability to be himself.

2.   Some particularities of the data on outer ionosphere sounding in the MIT region

by N P Benkova, E F Kozlov, N A Kochenova
Yu V Kushnerevsky, N I Samorokin and M D Fligel,
IZMIRAN, USSR

The results of simultaneous ground-based and satellite ionospheric sounding in complicated conditions are considered, ie in the zone of the main ionospheric trough (MIT), where isosurfaces of plasma frequencies are far from horizontal. The definition of the critical frequencies of the F2 layer using top-side ionograms is very difficult under these conditions. Top-side ionograms; for a horizontally homogeneous ionosphere are usually very clean in the band of operating frequencies f<foF2, as industrial and thunderstorm noises at frequencies <foF2 can not penetrate through the layer, and the frequency above which noise appears on the ionogram can be considered as foF2. At strong horizontal inhomogenities there arises a possibility of appearance of ground noises of f<foF2 on top-side ionograms obtained at heights > 700-800 km. A simplified scheme for the case of MIT (Fig. 1a) shows penetration of ground noise up to the altitudes of satellites.

There is also another difficulty in estimating the true foF2 using top-side ionograms, viz in the region of the MIT the equatorial wall of the N(h)-profile can be schematically represented as a wedge with the bottom surface being horizontal and the upper one - inclined. In this case ground-based sounding will give a correct value of foF2, but top-side sounding can give an underrated value of foF2 (see scheme Fig. 1b).
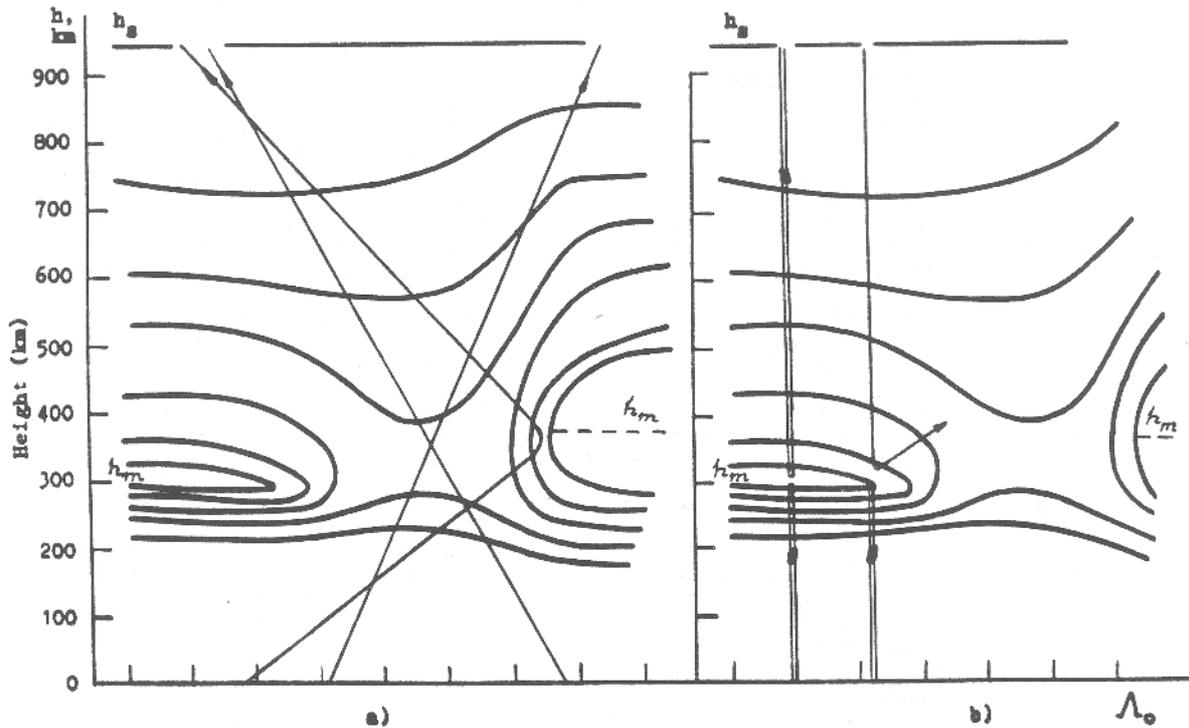

Fig. 1   A scheme of topside sounding in the region of main Ionospheric trough (MIT). The isolines of plasma frequencies are shown by curves.
a) Penetration of the interferences from the ground through the bottom of MIT to the heights $h > h_m$.
b) The trajectories of the sounding impulses.

To illustrate the above, Fig. 2a, b, c give the results of data processed from IK-19 [1] during its passes near the "ionospheric polygon" in the Arkhangelsk region (Arkhangelsk, invariant latitude Λ_o= 60°, Karpogory - 59°, Mezen - 61°). Fig. 2a shows data on foF2$_{sat}$ and plasma frequency at the satellite level (f_{os}) for winter evenings with a strongly manifested MIT and weakly perturbed magnetic field (Kp = 3), denoted by crosses. In the invariant interval Λ_o= 57-62°, corresponding to the equatorial wall of the trough, limiting frequencies f_{sat} are designated by points, up to which h'(f)-characteristics can be followed (thereafter it is very noisy). Values of foF2 using ground-based data (foF2$_{earth}$) are shown by stars. A star at Λ_o= 56° corresponds to Leningrad station, Λ_o= 64° to Murmansk; station Salekhard, marked by a solid cross at 60.6° is located 20° eastward from the polygon. Ground-based data are reduced to the local time of IK-19.

The agreement of foF2$_{earth}$ with foF2$_{sat}$ for stations Leningrad and Murmansk, the first located southward from the MIT, and the latter northward, in the region of anomalous ionisation, is very good. At the equatorial wall (stations Karpogory, Arkhangelsk, Mezen and Salekhard) foF2$_{earth}$ is considerably greater than foF2$_{sat}$ which agrees with the assumptions about the influence of ground-based noises.

As an additional test of the results obtained, the information concerning f_{os} has been extrapolated to the level of h_m . It has been assumed that the outer part of the N(h)-profile is approximated by the exponent

$$N_m = N_e \exp [\beta(h - h_m)] \qquad\qquad\qquad (1)$$

from which it follows, for the height of the satellite, that

$$N_m = N_{os} \exp [\beta(h_{sat} - h_m)] \qquad\qquad (2)$$

Taking the ionosphere above Leningrad ($\Lambda_o = 56°$) as typical of the mid-latitude conditions and assuming that it is horizontally homogeneous, the value of β has been calculated using (2); values of N are defined by the equation

$$N_m = 1{,}24 \cdot 10^4 \, (foF2)^2_{earth};$$

$foF2_{earth}$ and f_{os} were taken from the graph Fig. 2a; h_m is assumed to be equal to h_p, which was obtained from tabulated data for Leningrad station. The value $\beta = 0{,}0058$ thus obtained has been used in the calculation of $foF2_{sat}$ using formula (1) for latitudes of Arkhangelsk, Karpogory and Mezen, with the assumption that the vertical structure of the equatorial wall does not differ much from the mid-latitude structure. Necessary values of h_m have been taken from N(h)- profiles of ground-based stations. The small differences between extrapolated values of $foF2_{sat}$ (circles in Fig. 2a) and $foF2_{earth}$ has confirmed the usefulness of the assumptions made above. With the help of ground-based data the $foF2(\Lambda_o)_{earth}$ − profile is given in Fig. 2a by the dotted line. It shows greater steepness of the MIT equatorial wall and relatively narrow ($\approx 1{,}5°$) bottom of the trough.
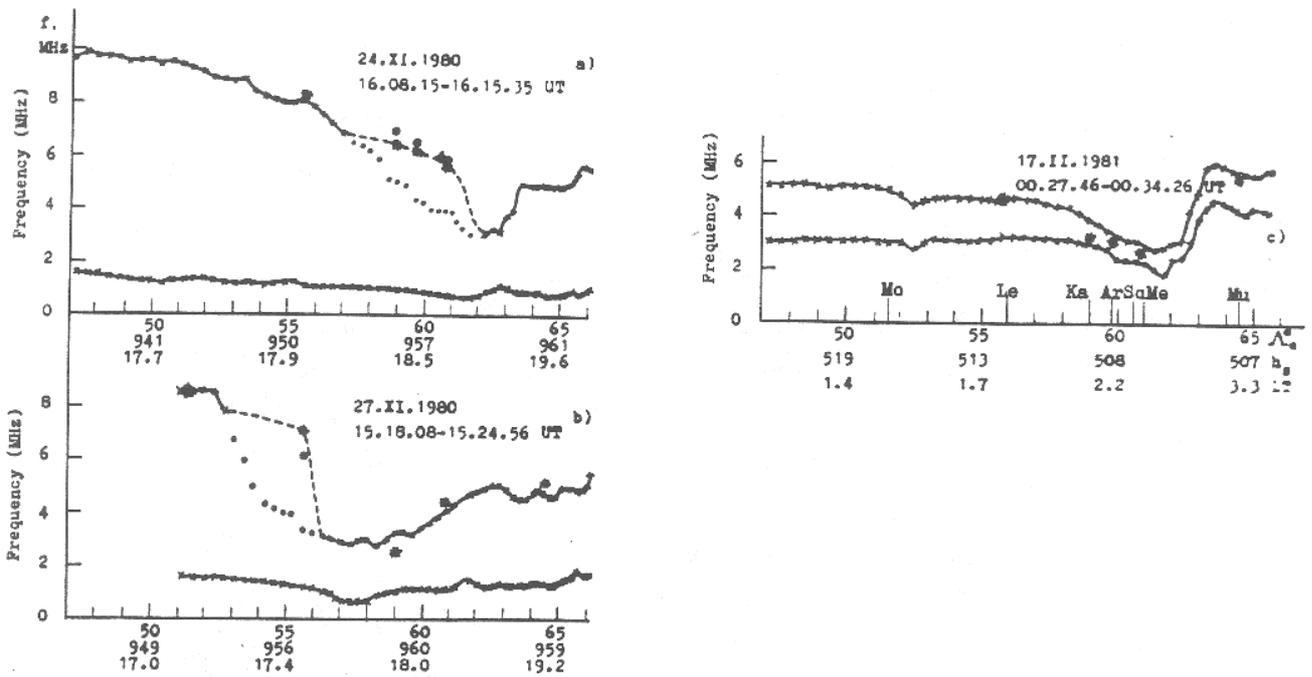

Fig. 2 Examples of the latitudinal dependences of $foF2(\Lambda_o)$, $f_{os}(\Lambda_o)$ The marking, notations and abbreviations are the following:

x   - corresponds to the measurements at the satellite;

*,+   - to ground-based data;

.   - to values of $foF2_{sat}$ determined according to the frequency at which the interferences from the
            ground appear at the ionograms;

o   - to the values of foF2 calculated according to f_{os};

Λ_o - invariant latitude;

h_s - the height of the satellite;

LT   - local time;

Mo - stands for Moscow, Le - for Leningrad, Ka - for Karpogory, Ar - for Archangelsk,
Sa - for Salekhard, Me - Mezen, Mu - Murmansk.

On Fig. 2a the data from Murmansk are not shown because of great diffusivity.

As was expected, foF2 was very much greater than f_{os}. A definite difference in the shape of latitudinal variation between foF2 and f_{os} is also revealed.

The second example (Fig. 2b), demonstrates the $foF2_{sat}$ - profile for the winter evening hours of a more perturbed day (Kp = 5), when MIT is shifted towards lower latitudes. In this case Leningrad is located at the MIT equatorial wall, Karpogory - at the bottom, Mezen and Murmansk - poleward of the trough, and Moscow (Λ_o= 51°) characterises the undisturbed mid-latitude ionosphere. The good agreement between $foF2_{sat}$ and $foF2_{earth}$ in the lower region of the trough indicates the relatively stable, horizontal structure of the ionosphere in this zone. The extrapolation of f_{os} to h_{max} level has been made for Leningrad by means of the value of β, defined for Moscow (value of β turns out to be equal to 0,0051 which is very similar to the above value obtained for Leningrad on 24.XI), and just like the case in Fig. 2a, the extrapolated value of $foF2_{sat}$ turns out to be close to the value of $foF2_{earth}$. In the lower region of the MIT, $foF2_{sat}$ in Fig. 2a and 2b are reliably computed. The satellite foF2(Λ_o) - profile in the region of the MIT equatorial wall has been corrected using the above information.

In both of the above cases described, the IK-19 orbit has been high enough and the difference in electron concentration at levels h_m and h_{sat} rather large. As the third example Fig. 2c shows the pass of the satellite at a smaller height (500 km), and reveals good agreement between the satellite and the ground based observations in middle, auroral latitudes and at the MIT equatorial wall. The reason being that ground noises of foF2 do not penetrate to this level.

Analogous comparison of ground-based and IK-19 based observations have been done for a large number of cases during different times of the day and different seasons, and the results obtained are the same as above.

The investigation allows one to make the following conclusions.

1. In the region of the MIT steep equatorial wall an underrating of f_{sat} can take place which is explained by the noises from industrial or thunder storm radiations or by variations of trajectories of the sounding signals in highly horizontally inhomogeneous ionosphere. Very careful analysis of satellite data are required if they are to be used in theoretical investigations or forecasting.

2. Extrapolation of plasma frequency from the level of the satellite to that of h_m turned out to be very successful. The extrapolation was achieved on the basis of the ionospheric exponential model using the parameters as defined by this model with the help of ground-based sounding data.

References

1. The apparatus for research of top-side ionosphere.
        Ed. IZMIRAN. M. 1980.

3.   Developing Ionosonde Usefulness

by Clarrie G McCue and John D Gilbert

Introduction

The IBM PC-XT computer has become widely used in recent years by scientific researchers as a valuable tool for data analysis. The engineers at KEL Aerospace P/L have always understood the operational value of computer control and processing and have developed a range of IBM PC-XT based systems in support of the widely used IPS-42/DBD-43 Digital Ionosonde. This article will outline some of the uses of these systems, with emphasis on the advanced ionospheric data handling capabilities that they provide.

KEL Uses IBM PC-XT Compatible Computers

The IPS-42/DBD-43 Digital Ionosonde produces digital ionograms stored on magnetic tape cartridges. The ionograms so recorded can be displayed and scaled using the normal functions of the DBD-43 operating firmware, and the storage of the analysed tapes for archival purposes is both efficient and very practical. Further use of the digitally recorded ionograms has previously been precluded by the understandable design limitations of the DBD-43 unit. The integration of the IBM PC-XT with the DBD-43 has made possible a wide range of ionospheric data analysis and manipulation capabilities which will prove useful for both ionospheric studies and real time radio wave propagation evaluations.

The IBM PC-XT supported KEL systems have two basic functions. The first is to transfer the DBD-43 digitally recorded ionograms to computer storage, and the second is to process and analyse the scaled data. These functions are explained further in the following sections of this article.

The Direct Tape Access Package

The Direct Tape Access Package consists of a PC-XT/DBD-43 interface card and appropriate software routines. It allows the transfer of the DBD-43 recorded ionograms to computer storage. The interface card actually connects to the Auxiliary Tape Drive

unit, which is a normal part of the DBD-43 Tape Duplication system. Software routines provide complete control of the tape drive, and ionogram transfer is fast and efficient. An ionogram is transferred in approximately two seconds. When the ionograms have been transferred they can be viewed directly on the computer screen, either individually or in a controlled sequence.

Additional Analysis and Processing Facilities

Another software package, called the Enhanced Ionogram Utilities Package, offers numerous data manipulation facilities. Since the ionograms are now stored on the PC-XT hard disk, file examination or tabulation is almost instantaneous. Ionograms scaled using the DBD-43 options can be displayed and text files of all scaled parameters can be generated. Fast printing is available together with file manipulation.

The KEL TIDPLOT routines are included in the Enhanced Ionogram Utilities software. These allow time-lapse image and file generation for a single frequency of range of frequency channels from a series of ionograms. The result is a picture of the ionospheric conditions for the selected frequency or range of frequencies throughout the sounding period being examined. Using this TIDPLOT the operational characteristics for a particular communication channel can be assessed, ionospheric disturbances are also easily studied together with gravity wave identification.

The KEL-48 Data-base and Report Generations System

The KEL-48 system has been used to generate monthly reports from the DBD-43 ionogram scalings, using serial data transfer directly from the DBD-43 unit. Several major improvements have been made now to the KEL-48 system allowing complete integration with the IBM PC-XT stored ionograms and data. Reports can be made now using the data stored in the computer, reducing the data manipulation time enormously. Semi automatic ionogram scaling is an additional feature of the KEL-48, this is achieved using an on-screen mouse cursor and menu driven scaling commands.

Automatic Ionogram Scaling

The most exciting IBM-based development is the Special Mid-latitude Automatic Real-Time Ionogram Scaling Technique software package (SMARTIST). This suite of software routines is designed to run on a standard PC-XT or compatible computer and automatically scale DBD-43 digital ionograms stored on hard disk.

SMARTIST scales standard IPS-42/DBD-43 ionograms without the need for O-wave and X-wave component separation or identification electronics. This has been made possible by the use of special scaling ,algorithms developed by KEL scientists. An antenna polarization unit will be available soon for use with the IPS-42/DBD-43, improving the performance of SMARTIST, especially for high-latitude stations.

The parameters currently being scaled using SMARTIST and typical scaling accuracy results are detailed in the accompanying table, the ionograms; used were from a standard IPS/DBD Digital Ionosonde without O/X-wave separation. These results have been obtained by comparing the SMARTIST scalings with manually scaled ones, using 300 ionograms recorded at Camden near Sydney in 1987. Column 1 of each section of the table denotes the parameters being scaled. Row 1 of each section indicated the magnitude of the manually scaled value of the parameter minus the automatically scaled one. The figures in the body of the table are the percentages of occasions when the differences were the value indicated. It can be seen that the full standard parameter set is not covered in these results. However, when SMARTIST is released later this year, all parameters will be scaled. A true height-electron density profile, based on POLAN techniques, will also be able to be produced using SMARTIST for each ionogram held in store.

TABLE

PERCENTAGE OF OCCASIONS WHEN MANUAL MINUS AUTOMATIC SCALING RESULTS WERE THE VALUE INDICATED

DIFFERENCE IN MHz

	-0.5	-0.4	-0.3	-0.2	-0.1	0	0.1	0.2	0.3	0.4	0.5	+/-0.5
fmin	0.0	0.4	1.2	5.8	36.4	53.1	1.9	0.4	0.0	0.0	0.0	0.8
foE	0.4	0.0	0.4	1.2	74.0	3.1	10.4	4.3	1.5	0.4	0.0	4.3
foEs	0.4	1.2	1.2	9.3	53.1	1.5	3.5	2.3	1.2	0.8	0.0	25.5
foF2	3.1	8.1	8.5	25.1	41.8	1.2	8.5	0.4	0.0	0.8	0.0	2.3
fxF2	4.7	7.7	12.7	26.3	41.0	1.9	1.5	0.4	0.0	0.0	0.0	3.5
fxI	0.4	1.2	6.6	27.1	60.0	1.2	1.5	0.0	0.0	0.0	0.0	1.9

DIFFERENCE IN Km

	-20	-15	-10	-5	0	5	10	15	20	+/-20
h'E	0.0	0.4	0.0	67.4	10.0	18.2	0.4	0.4	0.0	3.1
h'Es	0.0	0.0	0.0	17.0	31.0	35.2	5.0	0.8	0.0	10.8
h'F	0.8	0.8	17.8	51.9	5.0	1.5	1.5	1.9	0.0	18.6

At this stage SMARTIST is being refined prior to general release. It must be stated that SMARTIST is not a development software package but is a fully automatic ionogram scaling system. It will reduce considerably the time and the tedium of scaling ionograms while retaining the accuracy required for most ionospheric studies. It will soon become an essential tool in the operation of real-time ionospheric propagation forecasting systems. A full report on SMARTIST will be available to this Bulletin later this year.

Anyone wishing to have further information on these developments or on their availability should contact one of the authors at KEL Aerospace P/L.

Clarrie G McCue is Chief Scientist at KEL Aerospace Pty Ltd.

Jon D Gilbert is Manager of the Ionospheric Systems Division at KEL Aerospace Pty Ltd

KEL Aerospace Pty Ltd
111 Station Street
Malvern VIC. 3144
AUSTRALIA

Tlx: AA 152300
Phone Australia   (61) 3 500 0100
Facsimile   (61) 3 509 4005

4.   Information about the E-F valley region, from Ionograms

by J E Titheridge

Physics Department, The University of Auckland,
        New Zealand

At the INAG meeting in Tel Aviv a resolution was adopted that "the following profile parameters be determined wherever accurate profiles are measured:

(i)   the E-F valley depth;

(ii)   the height of minimum electron density in the valley and the upper valley boundary;

(iii)   the ratio of the F2 half peak density height to the peak height hmF2; and

(iv)   the height at foF1".

These parameters are desirable, to define the real height profile. For profiles calculated from ionograms, however, much of this information is just not available.

Broken lines in Figure 1 show the virtual heights for the ordinary ray (h'o) calculated from a model real height profile at a dip angle of 67°. Continuous lines show 3 of the infinite number of real-height profiles which will produce, exactly, the same values of h'o. The thick line (a) is the monotonic result, obtained when we assume that there is no valley between the layers. This gives a lower limit to the possible heights for the F layer. Profile (b) includes a valley with a width of 50 km (from the E layer peak to the upper valley boundary), while profile (c) has a valley width of 90 km. As the valley width increases the calculated gradients (dfN/dh) in the lower F region increase, so that the virtual heights h'o are not altered. The wide range of possible solutions, above the E layer peak, shows that none of the parameters in (i) to (iv) above can be determined with useful accuracy when data is available for the ordinary ray only.
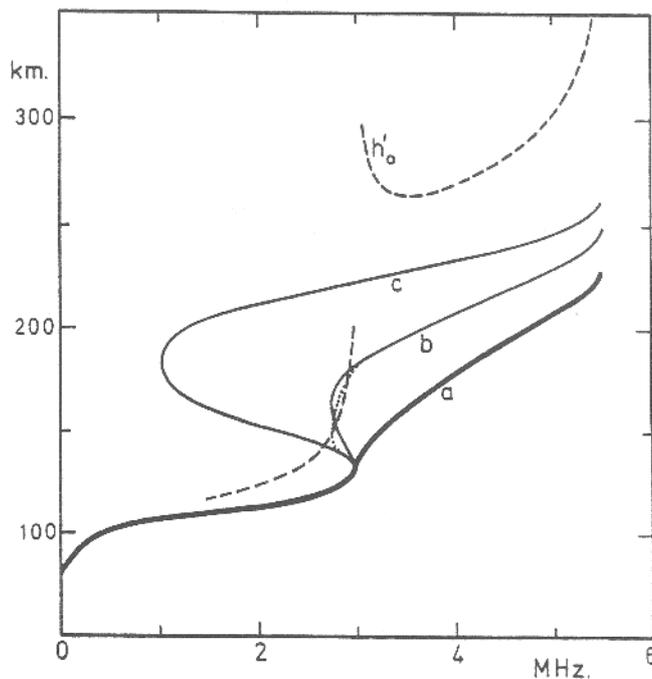
8

Fig. 1 Three real-height profiles(continuous lines) giving the
same virtual heights for the ordinary ray (broken lines).

The three profiles in Figure 1 do give different virtual heights for the extraordinary ray, at frequencies above foE. Thus from an analysis of combined ordinary and extraordinary ray data we can distinguish between the profiles a, b and c. We cannot, however, distinguish between the continuous line profile (b) and the variation shown by the dotted line. These two profiles have the same amount of ionisation in the valley region, and the same valley width at all plasma frequencies less than foE, so that they have the same effect on rays reflected from the F region. This makes it impossible to determine the height of minimum electron density, as required by (ii) above.

At dip angles of 26 to 30° ionogram data contains little or no information about the valley region, although the real heights in the F region can still be determined (Titheridge, 1974). At other dip angles we can often get reasonable estimates of the valley width, particularly for the small, shallow valleys which occur near noon, if we have good extraordinary ray data. Estimates of the valley depth are not possible if virtual-height errors exceed 0.1 km.

Larger valleys give larger errors in the calculated profile, due to uncertainties in the valley parameters. This is shown in Figure 2 which gives results for a model with a large valley, midway between curves b and c of Figure 1. Accurate values of h'o and h'x were calculated from this model, at a dip angle of 70°, and analysed using different assumed values for the valley depth. The valley calculation used 14 virtual heights (7 for each component), beginning at a plasma frequency of foE + 0.2 MHz, to determine the valley width and a 7-term polynomial representation of the lower F layer.
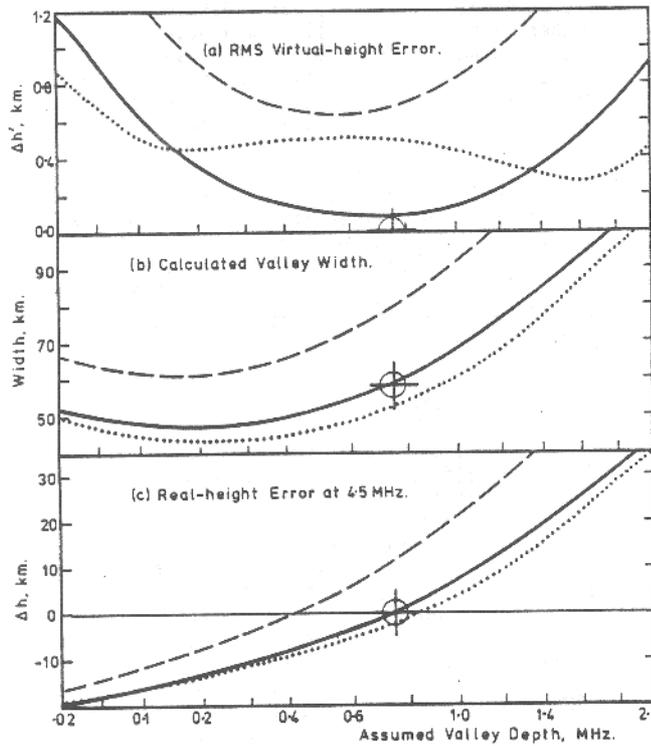
Fig. 2 Results obtained by analysing virtual-height data from a profile with foE = 4.0 MHz, using
ordinary and extraordinary ray data reflected at plasma frequencies of 4.2 (0.1) 4.8 MHz.
Continuous lines are obtained with exact data, using different assumed values for the valley
depth. Dashed and dotted lines are obtained with the inclusion of typical errors.

The accuracy with which the analysis fitted the virtual height data is shown by the continuous curve in Figure 2(a), as a function of the assumed valley depth. The fitting error never becomes zero, because of differences between the true valley shape and the model used in the analysis (described in Titheridge, 1985). The continuous line in Figure 2(b) shows the calculated valley width, using exact virtual height data, as a function of the assumed depth. (c) gives corresponding results for the real height at a plasma frequency of foE + 0.5 MHz. The targets in Figure 2 correspond to the correct values of depth (0.75 MHz), width (58 km) and height.

Calculations of the valley depth rely basically on determining the position of the minimum in the virtual-height fitting error. With errors of less than 0.25 km in h'x − h'o, estimates of valley depth range from about 0.6 to 1.0 MHz and heights in the lower F layer are accurate to about +5 km.

There is often a consistent error between scaled values of h'o and h'x due to the different strengths of the echoes and to horizontal displacement of the reflection points. The widely used IPS-42 ionosonde has a resolution of 3.2 km, and measurement errors will commonly exceed this. Dashed lines in Figure 2 show the effect of adding a fixed error, of +4.0 km, to the extraordinary-ray data. This increases the calculated valley width by 22 km, and the calculated height at 4.5 MHz by 12 km, when the correct value of valley depth is used in the analysis.

Frequency dependent errors can have a more serious effect. The dotted lines in Figure 2 show the results obtained when errors of +2, +2, 0, 0, -1, -1, -1 km are added to the 7 values of h'x used in the valley calculation. Errors of at least this size are inevitable in data scaled from film ionograms. Similar errors are likely with digital ionosondes because of changes in echo amplitude and horizontal deviations in the ionosphere. If the correct value of valley width is used in the analysis, Figures 2(b) and (c) show that the errors in calculated valley width and in the F-layer heights are only a few km. Figure 2(a) shows, however, that attempts to estimate the valley depth from such data can give results ranging from about 0.1 to 1.8 MHz. Calculated real heights in the lower F region then vary over a range of about 50 km.

From this discussion we conclude that the parameters (i) and (iia), called for in the Tel Aviv resolution can never be obtained from ionosonde data. Parameter; (iib), corresponding to the valley width, can be determined only from the best digital ionograms, and even so errors of the order of 50% (in valley width) will be common. We should therefore use model values for the valley depth under most conditions. Parameters (iii) and (iv) relate to heights in the lower F region. These will have errors which are typically two or three times the error in (h'x − h'o). Since virtual height errors are generally several km, due to ionosonde limitations and ionospheric irregularities, we must expect real height errors of about 5 to 15 km at the base of the F region. Possible errors will be much larger when (as in most cases) good data are not available from the extraordinary ray at frequencies approaching foE. To minimise these errors we need improved models for the depth of the valley, under different conditions; this is currently being studied by URSI working group G.4 on Ionospheric Informatics.

References

Titheridge, J E (1974), Direct analysis of ionograms
at magnetic dip angles of 26 to 30 degrees. J.
Atmosph. Terr. Phys., 36, 575-582.

Titheridge, J E (1985), Ionogram analysis with the
generalised program POLAN. Report UAG-93, World Data
Center A for Solar-Terrestrial Physics, NOAA, E/GC2,
Boulder, CO 80303.

5.   Polar F Region Lacunae, An Empirical Characterization

by Suzanne Cartron and Paul Vila

CRPE/CNET, 92131, ISSY, France

In this paper we would like to define simple and efficient rules by which to recognize and characterize F lacunae on polar ionograms. For this unexpected phenomenon the authors of the URSI Handbooks, otherwise thoroughly consistent in their rules, had to compromise between divergent opinions.

Also the scaling alphabet being exhausted, they were short of a specific symbol to characterize lacunae. The High Latitude Supplement (UAG-50, 1975) and the revised Handbook (UAG-23, 1972) present examples of real lacuna omitted, and of the Y symbol used without lacuna ("strong tilt cases"). Therefore it Is probable that the concept of real lacuna needs clearing up for many scaling persons; having compared series of records with their hourly tabulations or f-plots we believe that unequivocal lacuna recognition criteria are practicable and necessary, and that they require only slight changes in the polar ionogram scaling procedure.

Only with such changes could aeronomists be able to use the wealth of information contained in polar ionograms.

Lacunae are easily distinguished from gaps in F layer traces due to D layer or deviative absorption, to sporadic E occultation or to faulty sounding. Scaling will be simpler (and discussion also) if we reserve the Y symbol for unexplained trace disappearance. When because of this the three classical parameters of an F layer are replaced by the Y symbol, the layer (whether F1 or F2) should be marked as fully (or "truly") lacunated. When both layers are fully lacunated, an F3 lacuna should be indicated.

Here we will first discuss the ambiguities found in the Handbooks and propose a simpler definition and scaling procedures in accordance with it. We will then mention the lacuna scaling difficulties and the method to solve them, taking advantage of the easier trace readability of the Dumont d'Urville ionograms.

a) The 1972 URSI definition

F lacunae, a distinctive feature of the high latitude ionosphere, have been recognized by the international community since 1972 (URSI Commission 2, WARSHAW). The description of lacunae given in the URSI Handbook (revised edition, UAG 23A, July 1978) for ionogram scaling and interpretation is rather perfunctory. Section 2.75 summarizes: "Lacuna situations arise ... when traces which are normally reflected from a certain range of true heights disappear although the remaining trace show that the absorption is either normal or only slightly increased".

The recommendations which follow warn us against confusing real lacuna with echo vanishing which can be due to absorption, occultation, stratification or abnormal spreading. In the first instance the symbol Y is used while the others are noted by the usual B, R, A, H and F symbols. This caution is fully justified.

On the other hand, Section 3.28 of the Handbook's comment on the use of the Y symbol for "a lacuna, or a strongly tilted layer" is unfortunate because it overlooks the actual trace pattern, leaving the description insufficiently clear, which is dangerous. Also, it confuses under symbol Y two different situations, namely the true lacunarity which is an absence of trace (Figures 3.31 and 3.32). and a strongly tilted layer which brings additional traces (Figure 3.34). This amalgamation deprives the lacuna of a specific description and can hinder comparative studies on a global scale.

b) A more objective definition

Symbols A, B, R, G or even C correspond to perfectly morphological situations, quite distinct from one another, although they all show a disappearance of the expected traces. The Y symbol is also an indication of trace disappearance; as with the others we must be guided by the morphology of the traces remaining, not by theoretical assumptions about the traces absent.

Thus it seems to us reasonable to restrict the use of the Y symbol to clearcut cases where, all or part of an F layer trace, either F1 or F2 or both together, disappears without absorption (estimated on fmin) or occultation (evaluated from fbEs caused by a definite

sporadic E-trace) to account for it. When only F1 or F2 disappears we have a single lacuna L1 or L2; when they disappear simultaneously, a total F3 lacuna, or L3.

c)   F2 lacuna interpretation

The F2 lacuna or L2 case poses no difficulty if one limits oneself, as already explained, exclusively to observing and identifying the remaining traces (figure 1c). Here the difficulty lies in interpreting this F2 lacuna; the debate, more theoretical, will be presented in a later section, but it should in no way influence our scaling of the F2 lacunae. The "G situation" as described by the Handbook (3.1 letter G) is only one among various possible causes to account for missing F2 traces and must not be used a priori. The scaling parameter therefore reduces to the Y symbol by itself and should not come with any numerical value, unless a following-minute high gain record yields a clear measurement for foF2 which would be noted:--IY; this indicates clearly the absence of a G situation.

However if a sufficiently short interval record sequence (five minutes or less) indicated an foF2 decrease to less than foF1 followed by a subsequent increase, it would naturally become justified to specify foF2 = foF1 EG. At Dumont d'Urville such evidence for G is exceptional (less than 10^{-3} of the F2 lacuna occurrence).

d)   Practical tabulation with the Y symbol; full lacuna and lacunarity

The three routine parameters:

- h' for the lower frequency end

- M3000 for the mid-frequency band

- fo for the peak frequency,

can be affected by the Y symbol if the echo is missing on the corresponding frequency band and that the proper scaling symbol is not A, B, R, F, H (nor N, C either).

The extent of lacunarity depends on the number of parameters affected.
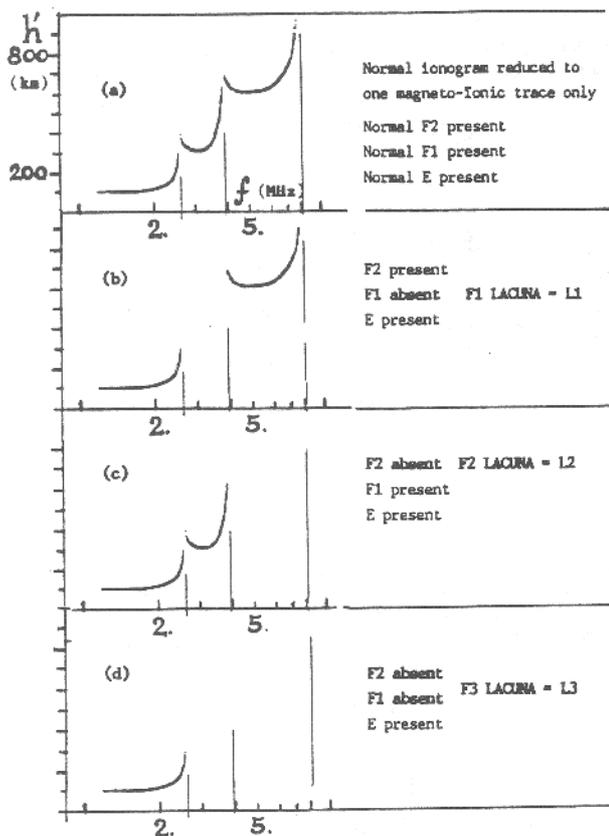

Fig. 1 Simplified ionogram and the three lacuna cases.

Real Lacuna. An F1 lacuna is present when and only when lacunarity is maximal for the F1 trace = all three parameters being replaced by Y, case (b) in fig. 1.

Likewise, an F2 Lacuna is present when all F2 parameters are replaced by Y (case (c), Fig. 1).
When (b) and (c) occur simultaneously and all parameters across the F region are replaced by Y, this is the case of total or F3 lacuna, maximum lacunarity over the maximum-height range, case (d) in Figure 1.

Note. A seventh parameter, foE, may also be replaced by Y; the occurrence of foE = Y is very high during F1 lacuna events; this often arises without clear sporadic E. At Dumont d'Urville they are sometimes associated with Slant E conditions, but not very often.

Lacunarity - we propose to replace the term "Lacuna phenomenon" used by the URSI Handbook (3.2) by this new tem. Thus we can reserve the tem Lacuna to the cases just described as those which show a maximal degree of lacunarity over a given F layer extent (the scaling tables keep a record of this partial lacunarity when it does not fulfil the above criteria of degree and extent).

e) Can lacunarity be quantified?

On the basis of these precise criteria it becomes possible to quantify the occurrence of the various lacunae and to define a numerical index (to be proposed in a later communication). If we succeed in our proposal, this index may become an independent tool for tests, even if these are limited, of the various theoretical models hitherto proposed and of future interpretation for the lacuna phenomenon.

Prospects and an appeal to those interested

We hope these modest amendments to the lacuna scaling procedure will be useful to the High Latitude community.

We would like to hear from groups or individuals interested in lacunae either from the angle of practical scaling or from that of either propagation or aeronomy.

The site and the ionosonde setup at Dumont d'Urville provide us with frequent lacuna events (on hourly results only, an average of over one per day for September and March and over four during November to February). We would like to know how frequently they are observed elsewhere, and whether other people would agree to correlate their results with ours.

We would be glad to receive this information, as well as any questions or comments through the INAG Bulletin, or directly, to:

Mme S Cartron, c/o INSU
4 Avenue Neptune
94 107 SAINT MAUR CEDEX, France

6.   Polar F Lacunae, Part II, An Occurrence Index

by Suzanne Cartron and Paul Vila

1. Characterizing lacuna occurrence
F lacunae are very frequent on ionograms of polar cap regions (Sylvain and Cartron, 1979) but show widely different occurrence from one day to the next. They only occur during Summer daytime except for a few rare cases.

Lacuna on classical ionosonde records is rather a qualitative feature since its existence is largely determined by receiver gain. The conventional three stepped gain successive records on the round UT hour often show complete traces on the high-gain ionogram, some lacunarity on the medium gain record and an apparent lacuna on the low-gain ionogram.

It has been difficult in the past to discuss lacuna occurrence. A Lebeau (1965) studied the hourly data and J Vassal (1971) quarterhourly series at Dumont d'Urville. Both these schedules are too discontinuous to show how lacunae come to appear and disappear and they allow us to identify less lacunae than high resolution runs do. M C Lecomte (unpublished) has analyzed one-minute sequences during November-December 1975: her results confirm the need for more high-resolution runs.

Our basic material remains the hourly ionograms.

Hourly F region parameters, if properly scaled according to the principles of Paper I above show certain days to be highly populated with all types of lacunae while others-have none. This marked day-to-day fluctuation has led us to define a daily index, the departure of the actual number of lacunae for the given day from a simple estimate of the probability of lacunae for the same day.

Leaving interpretation for further work, we merely describe here a method for obtaining a daily occurrence index and we give some examples of its use at Dumont d'Urville in 1980 - 1981.

2. Counting F1 and F2 lacunae

If we want to avoid interpretation it is obvious that F1 and F2 lacunae must be taken as different forms of a single phenomenon. We should therefore consider them as such and not confine our study to the concomitant or total F3 = F1 + F2 lacuna cases; to do this would prejudge the issue, taking for granted that the F1 + F2 phenomenon is more "intense" than either the F1 or F2 ones. It would also deny the distinctive character of F1 and F2 lacunae whereas a long practice has convinced us of their remarkable specificity: both F1 and F2 lacunae can last for hours perfectly independently. This point has perhaps been the most worrying for research workers. It has led them either to restrict their sample to the F3 types (Lebeau 1962) or else to consider F1 and F2 lacunae as separate entities (Sylvain 1977).

Our option here is to retain nothing but the quality that the two morphologically distinct situations have in common as a criterion; we give the same statistical weight to L1 and L2 whether they occur separately or together. Thus an F3 lacuna counts for two events. We take the presence of a lacuna as indicative of the conditions in the ionosphere surrounding it, whatever the overhead electron density may be.

Further, finer analysis could be undertaken to produce a more gradual index. This would use all the seven hourly parameters which define lacuna. The present paper is a first attempt to attribute a numerical value to each Summer day, characterizing it exclusively by its lacuna occurrence.

3. The proposed ILj index

a) A daily estimate Ib On routine hourly ionospheric tables seven parameters indicate lacunarity; three for each F layer (h', M3000 and fo) and one for the E layer foE, since the peak frequency band of the E layer sometimes shows no reflection leaving a trace which looks like an "I-type sporadic E" (this led to confusions before the Y symbol was officially recognized for F lacuna states by the Warshaw URSI Working Group).

Table I represents a fictitious synoptic F region scaling for a Summer day. This type of tabulation is only found on scaling notebook sheets which are becoming less usual, but it can be reconstituted from the published individual parameter files.
The daily Ib index, an Integer, is obtained by counting the sum of L1 and L2 cases whether simultaneous or not but unmistakably complete, which are framed on Table 1.

In our example Ib=7.

This index must be noted for every day between Autumn and Spring equinoxes.

TABLE I

Example of scaling sheet and Lacuna count or daily basic index; here I_b = 7

Local Time	f_oE	h'F	f_oF1	$M_{3000}F1$	h'F2	F_oF2	$M_{3000}F2$	Lacunae
05	240	240	L	L	L	55	240	
06	250	230	38L	L	450L	52Y	225F	
07	270	230	38	350	Y	451Y	Y	Lac F2 or L2
08	300Y	220UY	40	Y	Y	Y	Y	L2
09	Y	Y	Y	Y	Y	Y	Y	L1 + L2 = L3
10	Y	Y	42	Y	Y	Y	Y	L2
11	Y	210	42UY	Y	Y	Y	Y	L2
12	350ZY	Y	41UY	Y	460Y	60Y	Y	L1

10

b) Seasonal variation in the Ib lacuna occurrence

From the list of Ib values defined above we can deduce monthly averages.

On Figure 2 for December 1980 this monthly basic index $IB = \dfrac{150}{31}$ which means

that in this month an average of five lacunae a day can be expected.

IB values vary smoothly from September (IB = 0) to a peak in December-January, down again to zero in April.

14

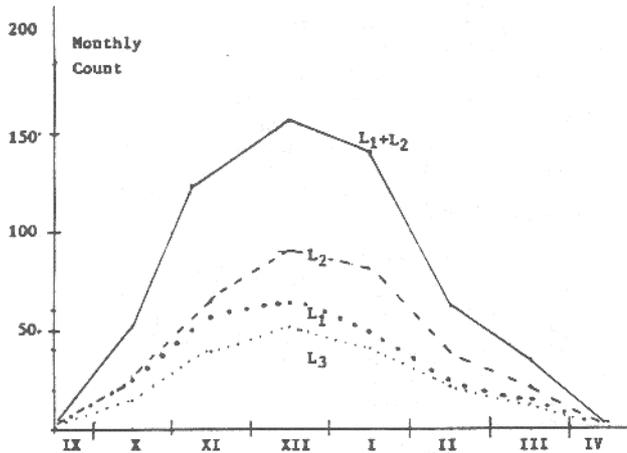Separate curves for the sub-types L1 and L2 show quite similar shapes peaking on December solstice.

Figure 2 . Seasonal variation

c) Basic daily lacuna index IBj

On figure 3 the IB curve can be easily smoothed, giving a linear IB variation between points centered at midmonths. Linear interpolation then yields a corrected integer value of the average IBj for each day.

On November 9 for instance the daily Ib was 6. The IB for November is 4. We want to characterize the daily value relative to the seasonally varying smoothed value IBj and not to the IB average: 4, while IBj ≈ 3.
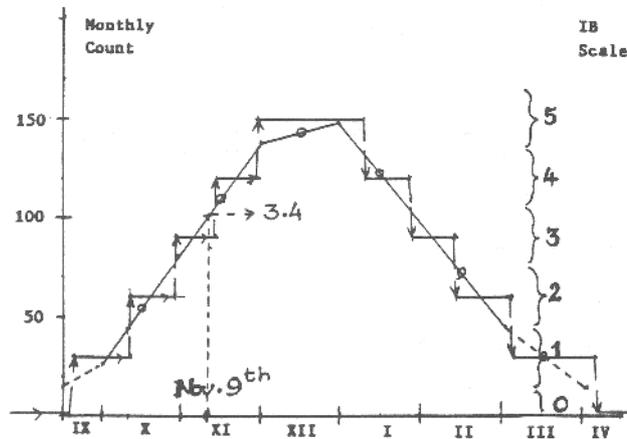
Figure 3 . Linearly normalized seasonal trend

On Figure 3 the successive intervals of days with the same integer IBj values for 1980-1981 are as follows on Table II.

Periods   IB interval   IBj
----
7 IV to 17 IX   0 <IB<0.5   0
18 IX to 11 X and 5 III to 6 IV   0.5<IB<1.5 1
12 to 28 X and 14 II to 4 III   1.5<IB<2.5 2
30 X to 13 XI and 26 I to 13 II   2.5<IB<3.5 3
14 to 29 XI and 9 to 25 I   3.5<IB<4.5 4
30 XI to 8 I   4.5<IB<5.5   5
----

d) The lacuna daily fluctuation index ILj

This is the difference between the daily occurrence Ib and the basic daily index IBj
ILj = Ib - IBj

15

ILj cannot fall below -5 since the maximum IB is 5. Negative ILj indicate lesser lacunarity than the average.

A quick glance at ILj values shows that their range of variation is maximum during the three solstitial months, whereas their monthly average is practically zero (except for November where ILj = $\frac{15}{30}$ = 0.5), and it justifies using integer values for IB, the ILj median value is approximately -1. This shows that ILj values vary more in periods of high lacuna occurrence than during weak lacunarity intervals.

The days selected for high lacuna occurrence are those with ILj in the top quartile of their month and the low lacunarity ones with ILj in the bottom quartile. The dates are given below for 1980 - 1981:

	Months	ILj	Dates
	Oct 1980	≥2	6,11,13,16,18,19,24,26,31
STRONG	Nov	≥4	12,19,21,26,28
LACUNA	Dec	≥4	1,12,13,15,16,20
OCCURRENCE	Jan 1981	≥5	23,29,30,31
	Feb	≥2	2,16,24
	Mar 1981	≥1	2,6,13,14
	Oct 1980	≤2	12,17,20,25,27,28,30
WEAK	Nov	≤3	2,3,5,6,23
LACUNA	Dec	≤5	4.5,17,23,24,25,27
OCCURRENCE	Jan 1981	≤4	10,16,18,20
	Feb	≤3	4,5,8
	Mar 1981	≤1	1,3,4

Table III

As there are days without lacunae, individual days can be much more crowded than the average. 15 December 1980, a rather quiet day, had 10 lacuna events; 20 December 1980 had 30.

- The LT dependence is decisive; dates on Table III are counted in UT + 9. It will be very useful to compare our ILj with those from other Antarctic ionosondes in order to track the spatial extent of lacunae; but this mapping should refer to neighbouring UT hours and to corresponding LT intervals. The daily scaling sheets are the only source of data for such comparisons.

- We also want to investigate the possible ionospheric features in the conjugate Arctic polar Cap areas during typical lacuna events in the Antarctic. Useful periods of fluctuating density of Lacunae are October 18 to 31, December 10 to 20 1980 and January 20 to 31 1981.

4)   Practical uses of ILj

Period selection

From a geophysical point of view it Is advantageous to investigate typical sequences; lacuna formation is best surveyed during succession of frequent and separate lacuna events. These are mostly populated with L1 and L3 types following periods of several days without lacunae.

On the other hand at Dumont d'Urville L1 types frequently arise on days with few lacunae during an Ap decrease after a period of blackout disturbance.

Another type with almost permanent lacuna conditions occurs when Ap has been consistently increasing for several days.

Thus for summer daytime periods, ILj tables are an easy tool for selecting typical days among the fluctuating response of the polar F region to the primary magnetospheric energy sources.

Main trends of ILj and Ap variations

The results of the 1980 - 1981 summer illustrated by Table 3 above provide some basic points.

a)   The 31 upper quartile days coincide with Ap maxima for 18 cases if we correct our daytime periods for proper <u>local time</u> (only for 12 cases if we use the improper UT interaval days). The other peak-ILj days have medium Ap activity*. These results have an immediate significance; the days of highest lacuna density occur in two different magnetic regimes; 60% among them (18) happen during substorm periods while the remaining 40% are quiet. This sole fact suggests a dual mechanism for lacunae, with a separate polar cusp source operating on the 40% crowded quiet days.

b)   The 29 lower ILj quartile days coincide with Ap minima for 13 cases in LT (11 cases in UT "days"). Weak ILj occur with $a_m \pi \bar{a}_m$ on 17 cases. These ratios leave about 30% days with <u>F1</u> lacunae during high Ap, and two days of weak ILj with strong a_m, 25 October 1980 and 10 January 1981. Thus the days of least lacuna occurrence divide into 60% with normally weak a_m activity, 33% with moderate a_m and two abnormal days of high a_m.

<u>Conclusions and outlook</u>

- On the local 500 km scale polar cap convection patterns have been shown to set the background for F region dynamics (Olesen, Stauning and Tsunoda 1986 and References therein). These convection patterns fluctuate in space and time. Therefore observations from one site alone cannot establish what the threshold conditions for lacuna formation may be; owing to the loss of information inherent to our lacunated records the best we can do is to observe the <u>initial</u> and <u>final</u> phases of typical lacunae on <u>rapid</u> ionogram sequences.

- We suggest that the <u>5 minute schedules</u> recommended during the World days of each month should be maintained and should be extended to special <u>Summer campaigns</u>. Data should be pooled internationally so as to map the lacunae over each polar cap network during some pre-arranged periods. This would also allow synoptic comparisons to be made with satellite electrodynamics and low-energy particle spectrometers. Polar cap - wide synoptics on the ground is necessary if we want to understand lacunae in relation to daytime polar arcs and patches and auroral lights. It would then become possible to test the present models of planetary scale Solar wind - magnetosphere - polar cap phenomena.

- However in the present limited scope of ILj indexing our first objective should be an <u>inventory</u> of all lacunae observed by the various ionosondes on the <u>hourly</u> records for the 1986 and 1987 summer periods, as defined in our paper I above. The easiest way to find lacunae is to use the daily sheets of hour-by-hour scaling as described in the Figure I of Paper I.

Anyone uncertain about lacuna detection and counting is warmly invited to send us ionogram enlargings, tracings and questions.

People interested in these studies but lacking the personnel to work out the tabulations are invited to send us copies of their daily sheets especially for the August - September 1986 Arctic series.

----

* Note - strangely these coincidences increase with a looser filter: $a_m \phi \bar{a}_m$ occur with strong ILj on 24 out of the 31 days.

REFERENCES

LEBEAU André 1965. Ann. Geoph. <u>21,</u> 1167.

LECOMTE-RIOUAIS M.C. 1976. "Rapid run F region characteristics November - December 1975 at DUMONT d'URVILLE" (unpublished).

OLESENS J K, P STAUNING and R T TSUNODA 1986. Radio Sci. <u>21,</u> 127.

PIGGOTT R and RAWER K 1972. "URSI Handbook of Ionogram interpretation and reduction", Rep. UAG. <u>23,</u> WDC A.

PIGGOTT R 1975. "High Latitude Supplement to the URSI Handbook on Ionogram", Rep. UAG. <u>50,</u> WDC A.

SYLVAIN M. "Etude du Phenomene Lacune-F..", These, 1972, Paris.

SYLVAIN M and CARTRON S 1979. Planet. Space Sci., <u>27</u> (W), 1293.

VASSAL J. "Etude de certains Phenomenes d'Absorptlon Ionospherique anormale..", These, 1971, Paris.

7.   Letters to the Editor

Dear Sir

 After reading INAG 51, I feel some explanation of the break-up of the New Zealand ionosonde chain is due to the ionospheric community.

The New Zealand Government has reduced funding for basic scientific research to about 75% of that for the financial year 1985-86. This has forced the research divisions within DSIR to decide which topics could still be supported from the basic grant and which would be required to be self funding.

The three ionosondes left in the chain (originally four but the Rarotonga Station was closed, due to lack of interest in its data, in 1984) were supported by the Director, Physics and Engineering Laboratory, but that support was withdrawn on 01 October 1986. The magnetic observatory, set up in Christchurch in 1903, was transferred to Geophysics Division on 01 April 1987. The Director of Geophysics Division was not willing to continue the ionosondes but agreed to give limited support whilst attempts were made to get financial support for the instruments.

The University of Canterbury, through its Physics Department, agreed to support the Scott Base ionosonde for, at least, the current year and, very importantly, provide an archival space for all the data and records taken on the NZ ionosondes since 1957. They have, since, agreed to store all the ionosonde records and data since recording began in the early 1940's. Thus the University will provide data and/or records for the meantime. It would be unrealistic to expect the continuation of a standard 15 minute programme with all hourly data extracted and published but the records are being read, in part, by the technician at Scott Base who received some training here before going South.

Both the ionosonde and the Askania three-component magnetometer were removed from Campbell Island and there is no prospect of reviving this station which had recorded on a variety of ionosondes continuously since 1942.

The third ionosonde, known variously as Belfast, Lincoln, Godley Head, Christchurch and, at present, Eyrewell, has been continuously producing records of the ionosphere since 1939. This is the unit which is now under threat of closure on 01 May this year. Geophysics Division has sustained the station whilst financial support was sought from a variety of sources but the Director, with the best will in the world, cannot continue to support the station after that date.

At the time of writing this letter, it seems that some financing has been secured and that the Eyrewell ionosonde will continue to produce vertical sounding records.
 C A Roper
 Technical Advisor
 Department of Scientific and Industrial Research
 Geomagnetic Observatory
 Geophysics Division
 Christchurch
 New Zealand

8.   Solar Eclipses for 1989

Partial Eclipse - 7 March 1989

The eclipse begins in the Hawaiian Islands, crossing northwestern North America, Greenland, extreme N E Asia, and the Arctic regions. Maximum magnitude 0.83. Eclipse begins at 1616.8 UT 17°N. 149°W, is greatest at 1807.7 UT 61°N, 169°W, and ends at 1958.2 UT 73°N, 44°W.

Partial Eclipse - 31 August 1989

The eclipse begins in the extreme southeastern Africa, crossing Madagascar and part of Antarctica. Maximum magnitude 0.63. Eclipse begins at 0333.6 UT 22°S, 40°E. is greatest at 0530.8 UT 61°S, 23°E, and ends at 0727.6 UT 74°S, 124°E.

9. International Geophysical Calendar
1989

(See other side for information on use of this Calendar)

Legend:

- (17) Regular World Day (RWD)
- (18) Priority Regular World Day (PRWD)
- [15] Quarterly World Day (QWD) also a PRWD and RWD
- [4] Regular Geophysical Day (RGD)
- [6 7] World Geophysical Interval (WGI)
- 6 + Incoherent Scatter Coordinated Observation Day
- [7] Day of Solar Eclipse
- [5 6] Airglow and Aurora Period
- 11* Dark Moon Geophysical Day (DMGD)

NOTES:

1. Days with unusual meteor shower activity are: Northern Hemisphere Jan 3,4; Apr 21-22; May 3-4; Jun 8-12; Jul 27-29; Aug 10-13; Oct 20-21; Nov 1-4, 16-18; Dec 12-15, 21-22, 1989; Jan 2-4, 1990. Southern Hemisphere May 3-4; Jun 8-12; Jul 26-30; Oct 20-21; Nov 1-4, 16-18; Dec 5-7, 12-15, 1989.

2. Solar Interplanetary Variability (SIV) Observing Program began in 1988 and runs through 1989, with in-depth data analysis in 1990.

3. Day intervals that IMP 8 satellite is in the solar wind (begin and end days are generally partial days): 29 Dec 1988-5 Jan 1989; 10-18 Jan; 24-30 Jan; 5-12 Feb; 18-24 Feb; 2-8 Mar; 15-21 Mar; 27 Mar-3 Apr; 9-16 Apr; 22-29 Apr; 5-11 May; 17-24 May; 30 May-6 Jun; 11-18 Jun; 24-30 Jun; 6-13 Jul; 19-26 Jul; 31 Jul-8 Aug; 13-20 Aug; 26 Aug-2 Sep; 7-15 Sep; 19-27 Sep; 1-10 Oct; 14-22 Oct; 26 Oct-4 Nov; 8-16 Nov; 21-29 Nov; 4-12 Dec; 16-24 Dec; 29 Dec-8 Jan 1990.

   There will not be total IMP 8 data monitoring coverage during these intervals. (Information kindly provided by the WDC-A for Rockets and Satellites, NASA GSFC, Greenbelt, MD 20771 U.S.A.).

4. + Incoherent Scatter programs start at 1600 UT on the first day of the intervals indicated, and end at 1600 UT on the last day of the intervals.

5. Incoherent Scatter world days: 890306-07; 890411-12; 890509-10; 890530-890604 LTCS; 890801-03 GISMOS; 890828-890901 WAGS; 891002-06 GITCAD and SUNDIAL; 891031-891101; 891127-28; 900125-29 GISMOS.

   where GISMOS= Global Ionospheric Simultaneous Measurements of Substorms;
   GITCAD= Global Ionosphere-Thermosphere Coupling and Dynamics;
   LTCS= Lower Thermosphere Coupling Study;
   SUNDIAL= Coordinated study of the ionosphere/magnetosphere;
   WAGS= Worldwide Acoustics Gravity Wave Study.

OPERATIONAL EDITION, September 1988   14

EXPLANATIONS

This Calendar continues the series begun for the IGY years 1957-58, and is issued annually to recommend dates for solar and geophysical observations which cannot be carried out continuously. Thus, the amount of observational data in existence tends to be larger on Calendar days. The recommendations on data reduction and especially the flow of data to World Data Centers (WDCs) in many instances emphasize Calendar days. The Calendar is prepared by the International Ursigram and World Days Service (IUWDS) with the advice of spokesmen for the various scientific disciplines.

The Solar Eclipses are:

a.) *7 March 1989* (partial) beginning in the Hawaiian Islands, crossing northwestern North America, Greenland, extreme N.E. Asia, and the Arctic regions. Maximum magnitude 0.83. Eclipse begins at 1616.9 UT N17 W149, is greatest at 1807.7 UT N61 W169, and ends at 1958.2 UT N73 W44.

b.) *31 August 1989* (partial) beginning in the extreme south-eastern Africa, crossing Madagascar, and part of Antarctica. Maximum magnitude 0.63. Eclipse begins at 0333.5 UT S22 E40, is greatest at 0530.8 UT S61 E23, and ends at 0727.6 UT S74 E124.

Meteor Showers (selected by P.M. Millman, Ottawa) include important visual showers and also unusual showers observable mainly by radio and radar techniques. The dates for Northern Hemisphere meteor showers are: Jan 3, 4; Apr 21-22; May 3-4; Jun 8-12; Jul 27-29; Aug 10-13; Oct 20-21; Nov 1-4, 16-18; Dec 12-15, 21-22, 1989; and Jan 2-4, 1990. The dates for Southern Hemisphere meteor showers are: May 3-4; Jun 8-12; Jul 26-30; Oct 20-21; Nov 1-4, 16-18; and Dec 5-7, 12-15, 1989.

Definitions:

Time	= Universal Time (UT);
Regular Geophysical Days (RGD)	= each Wednesday;
Regular World Days (RWD)	= Tuesday, Wednesday and Thursday near the middle of the month (see calendar).
Priority Regular World Days (PRWD)	= the Wednesday RWD;
Quarterly World Days (QWD)	= PRWD in the WGI;
World Geophysical Intervals (WGI)	= 14 consecutive days each season (see calendar);
ALERTS	= occurrence of unusual solar or geophysical conditions, broadcast once daily soon after 0400 UT;
STRATWARM	= stratospheric warmings;
Retrospective World Intervals (RWI)	= intervals selected by MONSEE for study.

For more detailed explanations of the definitions, please see one of the following or contact H. Coffey (address below): *Solar-Geophysical Data*, November Issue; *URSI Information Bulletin*; *COSPAR Information Bulletin*; *IAGA News*; *IUGG Chronicle*; *WMO Bulletin*; *IAU Information Bulletin*; *Solar-Terrestrial Environmental Research in Japan*; *Journal of the Radio Research Laboratories* (Japan); *Geomagnetism and Aeronomy* (USSR); *Journal of Atmospheric and Terrestrial Physics* (UK); *EOS Magazine* (AGU/USA).

Priority recommended programs for measurements <u>not made continuously</u> (in addition to unusual ALERT periods):

Aurora and Airglow — Observation periods are New Moon periods, especially the 7 day intervals on the calendar;

Atmospheric Electricity — Observation periods are the RGD each Wednesday, beginning on 4 January 1989 at 0000 UT, 11 January at 0600 UT, 18 January at 1200 UT, 25 January at 1800 UT, etc. Minimum program is PRWDs.

Geomagnetic Phenomena — At minimum, need observation periods and data reduction on RWDs and during MAGSTORM Alerts.

Ionospheric Phenomena — Quarter-hourly ionograms; more frequently on RWDs, particularly at high latitude sites; f-plots on RWDs; hourly ionograms to WDCs on QWDs; continuous observations for solar eclipse in the eclipse zone. See Airglow and Aurora.

Incoherent Scatter — Observations on Incoherent Scatter Coordinated Days; also intensive series on WGIs or Airglow and Aurora periods. Special programs: Dr. V. Wickwar, Utah State Univ., Center for Atmospheric and Space Sciences, Logan, UT 84322-4405 U.S.A., URSI Working Group G.5 (801)750-3641.

Ionospheric Drifts — During weeks with RWDs.

Traveling Ionosphere Disturbances — special periods, probably PRWD or RWDs.

Ionospheric Absorption — Half-hourly on RWDs; continuous on solar eclipse days for stations in eclipse zone and conjugate area. Daily measurements during Absorption Winter Anomaly at temperate latitude stations (Oct-Mar Northern Hemisphere; Apr-Sep Southern Hemisphere).

Backscatter and Forward Scatter — RWDs at least.

Mesospheric D region electron densities — RGD around noon.

ELF Noise Measurements of earth-ionosphere cavity resonances — WGIs.

All Programs — Appropriate intensive observations during unusual meteor activity.

Meteorology — Especially on RGDs. On WGIs and STRATWARM Alert Intervals, please monitor on Mondays and Fridays as well as Wednesdays.

Solar Phenomena — Solar eclipse days, RWDs, and during PROTON/FLARE ALERTS.

+++Solar Interplanetary Variability (SIV) — observations of transition phenomena solar minimum to solar maximum (1988-1989), with in-depth analysis in 1990. Contact Dr. E.J. Smith, JPL, MS169/506, 4800 Oak Grove Dr., Pasadena, CA 91109 U.S.A.

Space Research, Interplanetary Phenomena, Cosmic Rays, Aeronomy — QWDs, RWD, and Airglow and Aurora periods.

15